JOURNAL OF GEOPHYSICAL RESEARCH, VOL. 96, NO. D11, PAGES 20,831–20,839, NOVEMBER 20, 1991

Climatological Statistics of Stratospheric Inertia-Gravity Waves Deduced From Historical Rocketsonde Wind and Temperature Data

KEVIN HAMILTON

Geophysical Fluid Dynamics Laboratory/National Oceanic and Atmospheric Administration, Princeton University Princeton, New Jersey

Ten years of rocketsonde observations of wind and temperature in the 28–57 km height range at 12 stations (spanning 8°S to 76°N) were analyzed. The aim was to determine the geographical and seasonal variation of statistics relating to the propagation of inertia-gravity waves. As noted by earlier investigators, there is a clear tendency for the rocketsonde hodographs to display clockwise rotation with height in the extratropical northern hemisphere. This is consistent with the notion that the variations are dominated by inertia-gravity waves with upward energy propagation. By using the wind and temperature data simultaneously it was possible to determine a dominant direction of horizontal wave propagation for each profile. This quantity has an impressive seasonal variation in mid-latitudes, with strong eastward propagation apparent in summer and generally westward propagation in winter. This seasonal cycle is consistent with theoretical notions of how the mean flow ought to affect wave propagation. Two stations within 10° of the equator are included in this analysis. The results at these near-equatorial stations contrast strongly with those at higher latitudes. There is a clear tendency for the hodographs at these stations to display quite linear polarization (rather than the systematic rotation generally seen at higher latitudes). The wind variations also show a remarkable tendency to align themselves in the zonal direction. When the wind and temperature variations are used together, it can be shown that the variations seen are consistent with a clear dominance of eastward propagation.

1. Introduction

Indirect observational inferences [e.g., *Hartmann*, 1976; *Hamilton*, 1983; *Smith and Lyjak*, 1985] and results from simple theoretical models [e.g., *Lindzen*, 1981; *Holton*, 1982] suggest that inertia-gravity (IG) waves of less than planetary scales play a significant role in the general circulation of the stratosphere. It is quite clear that in at least some comprehensive general circulation models (GCMs) the vertical momentum transports associated with resolved IG waves are of critical importance in the simulation of stratospheric circulation [*Miyahara et al.*, 1986; *Mahlman and Umscheid*, 1987; *Hamilton and Mahlman*, 1988; *Hayashi et al.*, 1989]. (Also note that low-resolution GCMs apparently need a parameterization of gravity wave effects to produce a realistic stratospheric simulation [*Rind et al.*, 1988].) Direct observations of IG wave fluxes are difficult, and it is doubtful that current observations could establish the global climatology of, say, the IG vertical momentum flux divergence. However, the analysis of available observations is of interest, both to confirm the qualitative expectations based on theories of IG wave propagation and to provide detailed benchmarks for comparison with comprehensive model simulations.

One source of data with potential for studying IG waves is the archive of meteorological rocketsonde observations. Rocketsondes typically return data on temperatures and horizontal winds at roughly 1-km vertical resolution for the height range from about 30 km to about 60 km. *Hirota and Niki* [1985] were apparently the first to note that the hodographs produced from individual rocket soundings typically display a roughly elliptical polarization with clockwise (counterclockwise) rotation with height in the northern (southern) hemisphere. They noted that this corresponds to expectations if the wind field were dominated by a single plane monochromatic IG wave with upward energy propagation. In this simple case the orientation and eccentricity of the polarization ellipse would indicate the horizontal direction of propagation and the intrinsic frequency of the wave. *Hirota and Niki* [1985] made a statistical study based on an examination of several hundred hodographs from a number of stations to determine the sense of polarization and eccentricity, as well as a vertical amplitude profile. *Eckermann and Vincent* [1989] (following the work of *Vincent and Fritts* [1987]) used more objective analysis techniques applied to rocket measurements of the horizontal wind to study the climatology of IG waves over Woomera, Australia.

The present paper reports on an analysis of rocketsonde data covering a 10-year period at a number of stations throughout the world. The aim was to uncover any regular features of the stratospheric IG field in the climatological statistics of vertical wind and temperature variations. The analysis employed for the wind field was similar to (although less sophisticated than) that of *Eckermann and Vincent* [1989]. A novel feature of the present analysis was the use of both wind and temperature data. It will be shown that the derived statistics display a number of interesting systematic variations with season and latitude. The climatology created should be useful for comparison with results from general circulation models. Indeed, encouraging progress has been made in comparing a preliminary version of some of these rocket-derived statistics with comparable quantities computed from simulations produced by the Geophysical Fluid Dynamics Laboratory (GFDL) "SKYHI" troposphere-stratosphere-mesosphere general circulation model [*Hamilton*, 1988].

2. Data

The basic data employed were rocketsonde reports of horizontal winds and temperature for several stations for the

Paper number 91JD02188.

TABLE 1. Number of Rocket Profiles Employed

Station Name	Latitude	Longitude	Number of Observations	
			Summer	Winter
Thule	76.5°N	68.8°W	230	142
Chatanika	65.1°N	157.5°W	182	154
Churchill	58.7°N	93.8°W	217	326
Primrose Lake	54.7°N	110.0°W	214	175
Wallops Island	37.8°N	75.5°W	417	426
Point Mugu	34.1°N	119.1°W	429	530
White Sands	32.4°N	106.5°W	510	578
Cape Kennedy	28.5°N	80.5°W	421	399
Barking Sands	22.0°N	159.8°W	375	373
Antigua	17.2°N	61.8°W	221	202
Kwajalein	8.7°N	167.7°W	419	429
Ascension Island	8.0°S	14.4°W	366	366

period 1971–1980 provided by the U.S. National Climatic Data Center (NCDC) (their data set TD-5850). The data set included a total of 18,511 profiles from 20 stations. Inspection of many profiles showed that a small fraction appeared to have erroneous data at some levels (often the result of apparent keypunching errors). *Cayford and Hamilton* [1987] performed a quality control analysis which resulted in 101 profiles being discarded as likely erroneous.

For the present analysis the wind and temperature data at 1 km altitude intervals were extracted from the remaining profiles. Only soundings in which there were wind data reported at each level between 28 and 57 km, inclusive, were retained. Any profiles which had data at any of these levels flagged as "questionable" on the NCDC tapes were excluded. The vast majority of profiles with wind data from 28 to 57 km also had temperature data for the same levels.

The analysis described below required the computation of long-term mean profiles for individual months of the year. Thus attention has been restricted to the 12 stations that had at least 20 soundings during the 10-year period in each month of the year. These stations, along with the total number of soundings, are listed in Table 1. The numbers are given for both "winter" (November through April) and "summer" (May through October).

In discussing the results it will often be useful to distinguish three groups of stations: the "equatorial" stations (Kwajalein and Ascension Island), the "high-latitude" stations (Thule, Chatanika, Churchill, and Primrose Lake), and those for the remaining sites (Wallops Island, Point Mugu, White Sands, Cape Kennedy, Barking Sands, and Antigua) which will be loosely referred to as the "mid-latitude" stations.

3. METHOD OF ANALYSIS

3.1. *Preliminary Filtering*

The first step in the analysis at each station was a computation of 10-year mean wind and temperature profiles for each month of the year. Then the appropriate monthly mean was subtracted from each individual profile. The vertical mean (28–57 km) and the least squares linear vertical trend were then subtracted from each profile. The end result of all this manipulation is the raw material for the analysis to be discussed below, i.e., profiles each consisting of filtered u, v, and usually T values at 1-km intervals between 28 and 57 km. The filtering is designed to leave only those vertical variations caused by transient waves. Of course, the filtering will not work perfectly, since the long-term mean profiles are not necessarily determined with great accuracy from the available data and since any interannual mean flow variations can still contaminate the results. Two special concerns, namely the removal of atmospheric tides and the possible effects of the quasi-biennial oscillation on the results, will be addressed in the discussion in sections 8 and 9 below.

3.2. *Analysis for Individual Filtered Profiles*

Inspection of a large number of hodographs produced from individual filtered profiles showed that they typically display roughly elliptical polarization, with a clear dominance of clockwise rotation with height in the extratropical northern hemisphere. This is in agreement with the earlier findings of *Hirota and Niki* [1985]. Figure 1 shows an idealization of a purely elliptically polarized hodograph. This idealized hodograph would be observed if only a single harmonic plane IG wave were present. In this simple situation the major axis of the ellipse (denoted u' in Figure 1) would indicate the horizontal direction of phase propagation, although wave vector could be aligned either in the $+u'$ or $-u'$ direction.

Following *Eckermann and Vincent* [1989], a dominant direction, u', was determined for each profile by requiring that $\langle u'v' \rangle = 0$ and that $\langle u'^2 \rangle$ be greater than $\langle v'^2 \rangle$, where the $\langle \quad \rangle$ operator is an average over the 30 1-km levels. The dominant sense of polarization was determined by computing

$$\Psi = \langle u'(z)v'(z + 1 \text{ km}) - u'(z + 1 \text{ km})v'(z) \rangle.$$

The quantity within the brackets is the vertical component of the cross product of the horizontal wind vector at level z with that at the level 1 km above. If the wind rotates clockwise with height, this cross product is negative (i.e., down the z axis). The sign of Ψ was thus taken as an

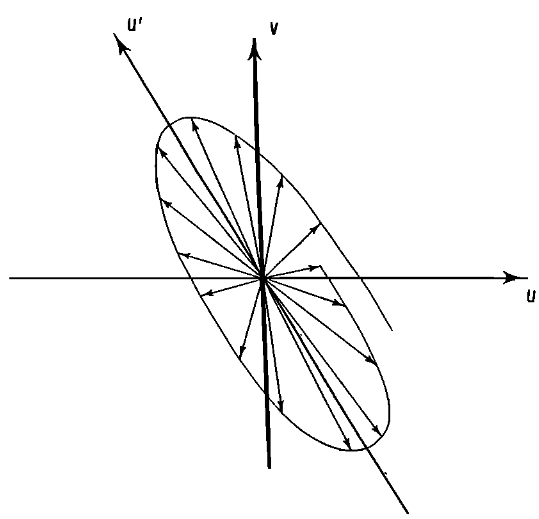

Fig. 1. An idealized hodograph showing an elliptically polarized oscillation that grows in amplitude with height. This shows an example of clockwise rotation with height. The u and v axes point eastward and northward, respectively. The u' axis is oriented along the major axis of the ellipse, and the v' axis (not shown) is aligned along the minor axis.

indication of the dominant sense of rotation for the entire profile. The results discussed in section 4 were found to be little changed if a somewhat different measure of dominant rotation were used, i.e., the number of levels for which the cross product with the level above is positive minus the number for which it is negative.

As noted by earlier investigators, the use of wind data alone can determine a dominant direction of propagation only with a 180° ambiguity. In the simple case of a single plane IG wave this ambiguity can be resolved by examining both the variations in u' and T' (see *Kitamura and Hirota* [1989] for one approach to this problem). It is easy to show that in this instance the wave perturbation T' and u' are in quadrature. However, the vertical derivative of T' will be either in phase or out of phase with u', depending on whether the wave horizontal phase velocity is parallel or antiparallel to the $+u'$ axis. Thus the dominant propagation direction for each measured profile was determined from the sign of the quantity

$$\eta = \langle u' T'_z \rangle.$$

Here the vertical temperature derivative T_z was computed using centered differences on the 1-km grid, and the average was actually performed only over the 28 levels spanning 29–56 km. While all the results reported below were based on the sign of η, very similar results were obtained when the direction of propagation was determined by computing the correlation of temperature with the vertical derivative of u'.

4. BASIC RESULTS

In this section some of the basic results concerning the mean properties of the hodographs at individual stations will be examined. Comparisons will be frequently noted with the earlier work of *Hirota and Niki* [1985] (hereinafter referred to as HN). HN computed similar kinds of statistics relating to IG amplitude, sense of polarization, and anisotropy, but all were based on subjective examinations of filtered hodographs. HN also adopted a very simple high-pass filtering (retaining only vertical wavelengths shorter than 15 km) of the raw hodographs to (hopefully) isolate the IG wave component. This contrasts with the present approach described above in section 3.1, which included removal of the long-term climatological mean wind profile.

Table 2 shows present determinations of the mean "winter" and "summer" amplitudes of both wind and temperature at each station. These values are simply the average over all available profiles of $\langle u'^2 + v'^2 \rangle^{0.5}$ and $\langle T'^2 \rangle^{0.5}$. The results suggest a tendency for higher IG wave wind amplitudes in the extratropics in winter than in summer and a tendency for larger amplitudes in low than in high latitudes, particularly in the summer. This appears to be consistent with HN's subjective amplitude determinations (see their Figure 3). The ratio of wind to temperature amplitudes in Table 2 is fairly constant, being ~3 m s^{-1} deg^{-1} everywhere except in the high-latitude winter results where it drops to about 2.5 m s^{-1} deg^{-1}.

TABLE 2. Root-Mean-Square Amplitudes for Filtered Profiles

	Wind Amplitude, m/s		Temperature Amplitude, °C	
Station Name	Summer	Winter	Summer	Winter
Thule	5.3	8.8	1.8	3.7
Chatanika	5.2	8.3	1.9	3.5
Churchill	6.2	8.8	2.1	3.5
Primrose Lake	6.6	9.3	2.1	3.5
Wallops Island	5.6	7.6	2.4	3.4
Point Mugu	6.0	7.9	2.3	3.5
White Sands	6.7	8.3	2.8	3.7
Cape Kennedy	7.8	7.7	2.9	3.3
Barking Sands	6.4	7.5	2.6	3.3
Antigua	8.7	8.7	3.0	2.9
Kwajalein	8.6	10.1	3.0	3.0
Ascension Island	9.6	9.9	2.8	3.0

TABLE 3. Sense of Polarization and Mean Anisotropy for Filtered Profiles

	Fraction Clockwise		Mean Anisotropy	
Station Name	Summer	Winter	Summer	Winter
Thule	0.98	0.90	2.4	2.5
Chatanika	0.90	0.81	2.9	3.7
Churchill	0.95	0.91	2.3	2.4
Primrose Lake	0.97	0.90	2.2	2.3
Wallops Island	0.91	0.80	3.0	3.1
Point Mugu	0.95	0.83	2.7	3.3
White Sands	0.95	0.80	2.6	3.0
Cape Kennedy	0.93	0.82	2.7	2.6
Barking Sands	0.90	0.78	2.9	2.9
Antigua	0.97	0.76	2.7	2.6
Kwajalein	0.77	0.54	4.1	4.8
Ascension Island	0.30	0.25	4.3	4.2

The first two columns in Table 3 give the fraction of profiles for which the dominant polarization was found to be clockwise with height as determined by the sign of Ψ. There is a strong dominance of clockwise polarization at all the high- and mid-latitude stations. At Ascension Island the only southern hemisphere station, there is actually a preponderance of counterclockwise polarization. These results are consistent with HN's summary based on their subjective determination of the dominant sense of polarization.

The third and fourth columns in Table 3 give the mean values of the anisotropy defined as

$$\mu = (\langle u'^2 \rangle / \langle v'^2 \rangle)^{0.5}$$

In the simple case of a single plane IG wave this would be the ratio of the intrinsic angular frequency of the wave to the local Coriolis parameter. *Eckermann and Hocking* [1989] warn against any simple interpretation of μ as an indication of dominant wave frequencies. In particular, they note that the random superposition of several waves with horizontal wave vectors oriented in different directions leads to low values of anisotropy in the resulting hodographs. Thus large values of μ may be taken as an indication of a tendency for the various wave components present to have some strongly dominant direction of horizontal phase propagation.

The values of μ seen in Table 3 are typically between 2 and 3 at all stations, except the equatorial stations where the mean μ is over 4 in both seasons. This change is readily apparent in subjective examinations of large numbers of profiles. At Ascension Island and Kwajalein there is a clear tendency for more linear polarization of the filtered hodographs than at the other stations. Figures 2 and 3 show histograms of the μ values for winter and summer at

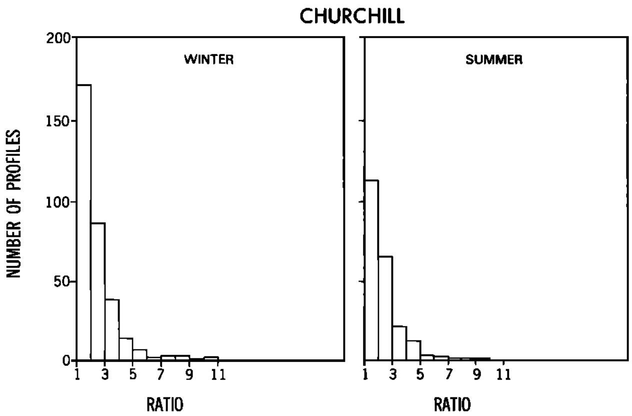

Fig. 2. Histogram of the anisotropy parameter for the profiles at Churchill in (left) "winter" and (right) "summer." See text for details.

Churchill and Kwajalein, respectively. The tendency for larger values of μ at Kwajalein is also quite apparent in these figures. *Hirota and Niki* [1985] quote typical values of anisotropy between about 2.5 and 5 and note a tendency for larger values at low latitudes.

The results presented in this section on amplitude, asymmetry, and sense of polarization have all shown that the general results of HN are reproduced with the objective analysis procedures employed here. In the next section some more novel results on directionality are reported.

5. Results on Dominant Directions of Propagation

For each profile for which both wind and temperature data were available a dominant horizontal direction of propagation was computed using the u' axis and the sign of η, defined above. Figures 4 to 9 are histograms of the resulting distribution of directions for each station in winter and summer. The results here have been binned into 20-deg intervals, and the normalization of the arrow lengths in each panel is arbitrary. The dominant propagation directions have impressive variations with latitude and season.

At the "mid-latitude" sites (Figures 6–8) the results have a very clear seasonal cycle, with strongly dominant eastward propagation in summer and a more isotropic distribution in winter (although with a distinct westward bias at Wallops Island, Point Mugu, White Sands, and Cape Kennedy). This general trend is in accord with theoretical expectations, since the strong mean easterlies (westerlies) in the summer (winter) lower stratosphere ought to filter out most of the waves with easterly (westerly) components of phase velocity. The results appear much cleaner in summer than winter. This may indicate that the filtering procedure employed more effectively isolates the IG wave component in summer, or it might reflect a real seasonal variation in wave propagation characteristics. The steady easterly flow in summer should be very effective in filtering out any waves with a westward component of phase velocity, while the more disturbed flow patterns of winter might at times allow a

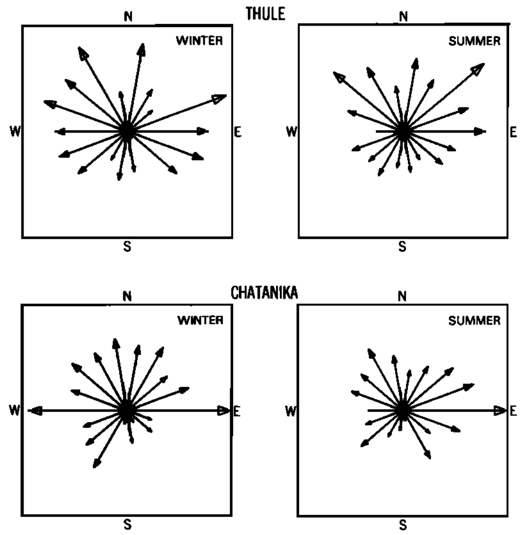

Fig. 4. Each panel gives the distribution of dominant directions for a particular station in either "winter" or "summer." The length of each arrow is proportional to the number of profiles that had dominant directions within plus or minus 10° of the arrow. The normalization of the arrow lengths from panel to panel is arbitrary. Results for (upper panels) Thule and (lower panels) Chatanika.

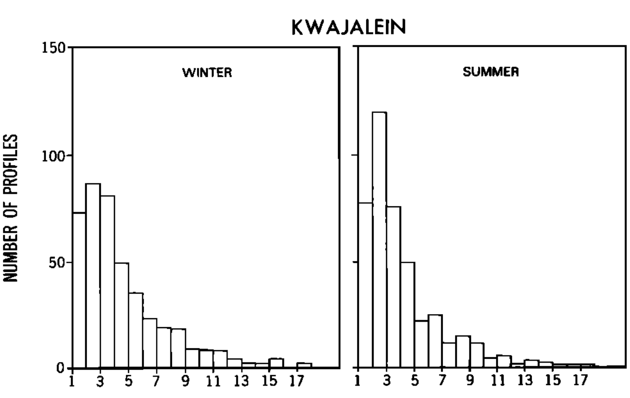

Fig. 3. As in Figure 2 but for Kwajalein.

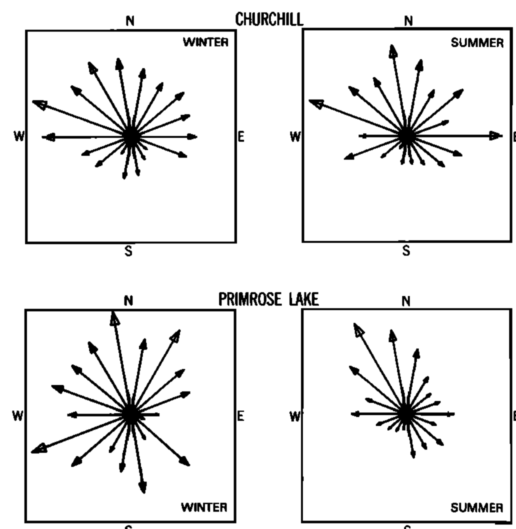

Fig. 5. As in Figure 4 but for (upper panels) Churchill and (lower panels) Primrose Lake.

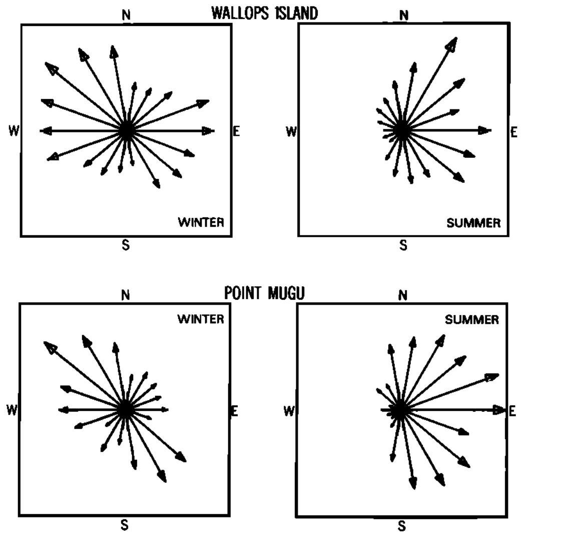

Fig. 6. As in Figure 4 but for (top panels) Wallops Island and (lower panels) Point Mugu.

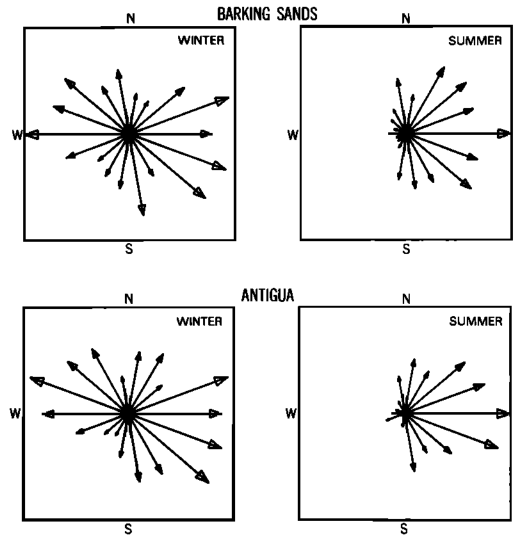

Fig. 8. As in Figure 4 but for (top panels) Barking Sands and (lower panels) Antigua.

greater fraction of eastward propagating waves to reach the upper stratosphere.

There is a clear tendency for poleward propagation in the mid-latitude sites. This is consistent with the findings of *Eckermann and Vincent* [1989] at Woomera (31.5°S).

The high-latitude sites (Figures 4 and 5) have much less seasonal variation. The most notable feature in the histograms for these stations is the dominance of northward propagation (even more pronounced than at the mid-latitude sites). This might suggest a low- or mid-latitude source for the IG waves that reach the polar upper stratosphere.

The most striking results are found at the equatorial stations (Figure 9). Here the dominant direction determined for the vast majority of soundings is within 30° of due eastward. An attractive explanation for this would be that the flow features seen in the rocketsonde profiles are dominated by equatorial Kelvin waves. This would also be in accord with the large values of anisotropy at these stations noted earlier (Table 3), since this is an indication of a single preferred direction for any waves present [*Eckermann and Hocking*, 1989]. It is important to emphasize that the results at Kwajalein and Ascension Island do not imply that only Kelvin waves are present near the equator. For pure Kelvin waves, one would expect very small values of meridional wind. The actual anisotropies at the two low-latitude sites are only a factor of about 1.5 greater than those at mid-latitude stations.

One complicating factor at low latitudes is the large zonal wind variation associated with the quasi-biennial oscillation. A simple attempt to reduce the influence of this mean wind oscillation on the present analysis is discussed in section 8 below.

Table 4 presents a station-by-station summary of the results on directionality. A "mean direction" was computed for each station by summing unit vectors, pointing in the preferred direction for each individual profile. A "collima-

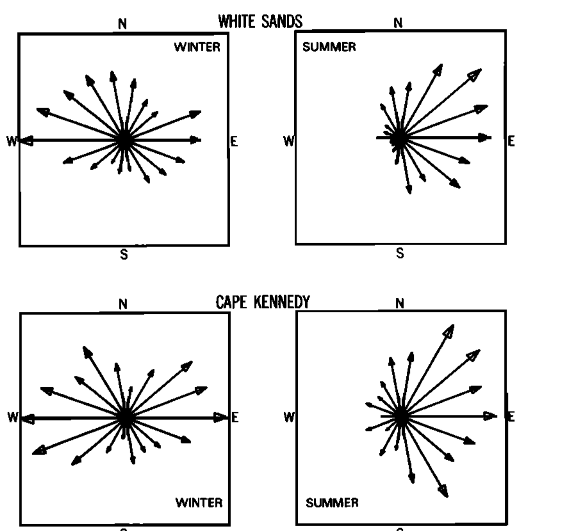

Fig. 7. As in Figure 4 but for (top panels) White Sands and (lower panels) Cape Kennedy.

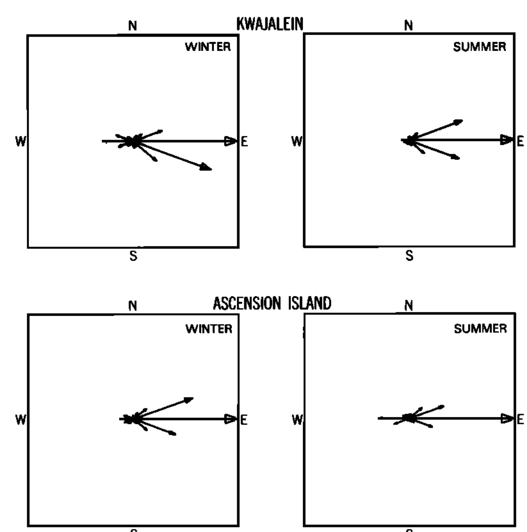

Fig. 9. As in Figure 4 but for (top panels) Kwajalein and (lower panels) Ascension Island.

TABLE 4. Mean Direction and Collimation for the Ensemble of Profiles

	Mean Direction (Degrees E of N)		Collimation	
Station Name	Summer	Winter	Summer	Winter
Thule	23	−15	0.16	0.12
Chatanika	38	−17	0.17	0.19
Churchill	−3	−23	0.21	0.23
Primrose Lake	−14	−44	0.24	0.17
Wallops Island	73	−24	0.42	0.14
Point Mugu	77	−24	0.30	0.10
White Sands	76	−27	0.31	0.10
Cape Kennedy	84	−66	0.38	0.10
Barking Sands	87	106	0.40	0.05
Antigua	85	68	0.51	0.09
Kwajalein	93	102	0.73	0.48
Ascension Island	82	87	0.44	0.62

tion'' was then defined as the length of the sum of the unit vectors divided by the number of profiles. This will be 1 if all profiles have exactly the same dominant direction or 0 for a randomly oriented set of profiles. The dominant eastward propagation at low latitudes and in summer at mid-latitudes is apparent from Table 4.

6. RESULTS FOR DIFFERENT VERTICAL SCALES

Eckermann and Vincent [1989] computed a number of vertical spectra and cospectra from their wind data, basing their approach on the Stokes' parameters of electromagnetic theory. A simpler approach with similar aims was adopted in the present study. After the initial filtering (see section 3.1), each profile can be decomposed into 15 vertical harmonics that are resolved by the 1-km data. Three filters were adopted to isolate particular vertical scale ranges: filter 1, including only the three harmonics corresponding to vertical wavelengths of 15, 10, and 7.5 km; filter 2 including the wavelengths from 6 to 4.3 km; and filter 3, which retained only wavelengths from 3.75 to 2 km. Tables 5–7 present various quantities computed from the filtered profiles for a high-latitude station (Table 5), a mid-latitude station (Table 6) and an equatorial station (Table 7). In each case most of the rms power resides in the 7.5–15 km wavelength range. The mean anisotropy, mean direction, collimation, and fraction of profiles displaying clockwise rotation with height are similar in each case whether filter 1 or filter 2 is applied, and the results are similar to those found from the full profile (Tables 3 and 4). This is supported by Figure 10, which shows the histograms of dominant propagation directions for White Sands and Cape Kennedy when filter 1 is used on the profiles. These plots are very similar to those based on results obtained with the full profiles (Figure 7).

TABLE 5. Comparison of Various Statistics for Profiles Subject to Different Filters

Statistic	Filter 1	Filter 2	Filter 3
rms wind amplitude, m/s	4.7	3.2	3.0
rms temperature amplitude, °C	1.72	0.98	0.76
Fraction clockwise	0.87	0.86	0.70
Mean anisotropy	4.5	3.9	4.3
Mean direction (degrees E of N)	−1	−4	−154
Collimation	0.24	0.16	0.01

Results for Churchill in summer.

TABLE 6. As in Table 5 but for White Sands

Statistic	Filter 1	Filter 2	Filter 3
rms wind amplitude, m/s	5.7	3.4	2.2
rms temperature amplitude, °C	2.14	1.39	1.12
Fraction clockwise	0.85	0.83	0.75
Mean anisotropy	4.2	3.8	5.4
Mean direction (degrees E of N)	77	81	156
Collimation	0.32	0.09	0.10

The results for the shortest wavelength waves (filter 3) in Tables 5–7 differ significantly from the longer wavelengths. When compared with filters 1 and 2, the collimation for filter 3 profiles is small and the fraction of clockwise profiles is low. Using Ascension Island rocket data, *Hirota* [1978] found that Kelvin waves dominated the fluctuations with vertical wavelengths greater than about 15 km. At shorter scales he found more isotropic disturbances. The present results are consistent with this general result but suggest that even at small vertical scales some residual preference for zonal orientation remains.

7. RESULTS FOR 3-MONTH SEASONS

The two ''seasons'' used in the various analyses reported above were chosen to represent roughly the period when mean easterlies fill the mid-latitude stratosphere (''summer'') and the period of mean westerly flow (''winter''). The calculations were also repeated for shorter seasons defined as December–February (DJF), March–May (MAM), June–August (JJA), and September–November (SON). The results for Churchill, White Sands, and Kwajalein are summarized in Tables 8, 9, and 10, respectively. It was found that most quantities that showed strong ''summer'' versus ''winter'' contrasts had even larger differences between DJF and JJA values. Thus, for example, the seasonal differences in rms amplitude at Churchill, while apparent in the ''summer''/''winter'' results in Table 2, are even more pronounced in the DJF and JJA results (Table 8). Similarly, the high ''summer'' values of collimation at White Sands (Table 4) are even higher when only the JJA period is considered (Table 9).

8. EFFECT OF THE QUASI-BIENNIAL OSCILLATION

The quasi-biennial oscillation (QBO) could affect the present results in two ways. The difference between any instantaneous wind profile and the long-term mean will

TABLE 7. As in Table 5 but for Kwajalein

Statistic	Filter 1	Filter 2	Filter 3
rms wind amplitude, m/s	7.6	3.5	2.1
rms temperature amplitude, °C	2.46	1.41	1.02
Fraction clockwise	0.67	0.74	0.59
Mean anisotropy	7.4	5.2	10.7
Mean direction (degrees E of N)	93	89	90
Collimation	0.60	0.52	0.30

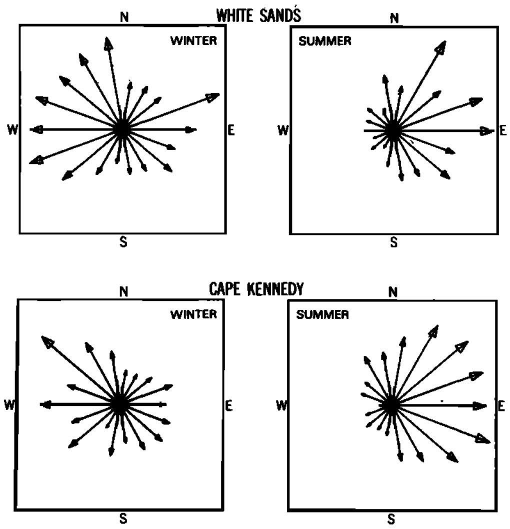

Fig. 10. As in Figure 7 but for using wind and temperature profiles that were filtered to retain only vertical wavelengths from 7.5 to 15 km.

depend to some extent on the phase of the QBO. Thus the profiles at the two equatorial stations after the processing described in section 3.2 are contaminated by a zonal wind and temperature component unrelated to the IG wave field. Fortunately, the QBO is known to drop off rapidly above 30 km altitude [*Reed*, 1965; *Hamilton*, 1981], but this effect may still be appreciable. In addition, the QBO mean wind variations presumably affect the nature of the actual wave field present in the tropical upper stratosphere.

In order to assess these effects the analyses at Kwajalein and Ascension Island were repeated but with attention restricted to that portion of the full 10 years that had easterly QBO phase. The easterly periods were judged from the 50 mbar winds as read from *Naujokat*'s [1986] time-height section of the monthly mean zonal wind at Gan (1971–1975) and Singapore (1975–1980). Note that the long-term monthly means removed in the initial processing of the profiles were also based only on the periods of mean 50 mbar easterlies. The results for winter at Kwajalein are shown in Table 11, along with results for a similar analysis restricted to westerly periods. The results are very similar in the westerly and easterly phases, with dominant eastward propagation and large values of mean anisotropy and collimation. Similar results were found in summer and at Ascension Island. It is also striking that the anisotropy and collimation are almost unchanged from those computed using all observations (Tables 3 and 4).

TABLE 8. Comparison of Various Statistics in Different Seasons Determined From Rocketsonde Profiles at Churchill

Statistic	DJF	MAM	JJA	SON
rms wind amplitude, m/s	10.2	6.8	5.3	7.5
rms temperature amplitude, °C	4.12	2.50	1.89	2.84
Fraction clockwise	0.87	0.99	0.95	0.89
Mean anisotropy	2.8	2.1	2.4	2.4
Mean direction (degrees E of N)	−49	53	25	−45
Collimation	0.37	0.22	0.31	0.34

TABLE 9. As in Table 8 but for White Sands

Statistic	DJF	MAM	JJA	SON
rms wind amplitude, m/s	8.8	7.1	7.3	7.1
rms temperature amplitude, °C	3.99	3.00	2.95	3.04
Fraction clockwise	0.74	0.94	0.94	0.92
Mean anisotropy	3.2	2.5	2.8	2.6
Mean direction (degrees E of N)	−13	40	68	84
Collimation	0.11	0.06	0.46	0.10

9. EFFECT OF THE DIURNAL CYCLE

The vertical variations in the wind and temperature measured in instantaneous wind profile includes a component due to the diurnal tide. Observations suggest that the amplitude of the diurnal wind oscillation at low latitudes and mid-latitudes could be of the order of 2 m s^{-1} near 30 km, rising to as much as 5 m s^{-1} near 60 km [*Reed et al.*, 1969]. Thus present results could conceivably by influenced by tidal contamination. Two factors limit the actual amount of this influence, however. In the extratropics the tidal variations have very long vertical wavelengths, and the removal of the mean and linear trend from each profile should largely filter out the tidal variations. Second, although rocket launchings do occur at various times of the day, at each station the large majority of profiles are grouped within about an hour of some particular time of day. Thus the calculated long-term mean, which is subtracted from the individual profiles, actually includes the tidal variation with the correct phase (for most of the profiles at least).

The most probable candidate for serious tidal contamination was Ascension Island, which is at low latitudes where the diurnal tide includes some reasonably short vertical scales and had the observations that were least localized in local time. In this "worst case" about 60% of the observations fell within 1200–1500 UT. Table 12 compares the results of the present analyses at Ascension Island when all the observations are used with those when data taken between 1200 and 1500 UT are employed. This should give some indication of the effects of the tides, since the results for the limited data set should have the tidal components more effectively removed. It is very reassuring that the results are so similar in the two cases.

10. CONCLUSION

Historical meteorological rocketsonde observations have been used to produce climatologies of wind and temperature variations in the upper stratosphere at 12 stations distributed over much of the world. Objective measures of the amplitude, anisotropy, and sense of polarization of individual hodographs were formulated. A very strong tendency for

TABLE 10. As in Table 8 but for Kwajalein

Statistic	DJF	MAM	JJA	SON
rms wind amplitude, m/s	10.8	8.5	8.8	9.0
rms temperature amplitude, °C	3.16	2.80	3.13	2.93
Fraction clockwise	0.44	0.71	0.82	0.68
Mean anisotropy	4.8	4.1	4.3	4.5
Mean direction (degrees E of N)	104	94	91	100
Collimation	0.44	0.64	0.75	0.62

TABLE 11. Various Statistics for Winter (November–April) at Kwajalein Computed Using Only Years of Easterly QBO Phase and Then Using Only Years of Westerly QBO Phase

Statistic	Easterly Phase	Westerly Phase
rms wind amplitude, m/s	9.8	10.1
rms temperature amplitude, °C	2.98	2.98
Fraction clockwise	0.55	0.56
Mean anisotropy	4.4	5.2
Mean direction (degrees E of N)	107	95
Collimation	0.43	0.51

dominant clockwise rotation with height is apparent in the extratropical northern hemisphere. Also noteworthy is a tendency for more nearly linear polarization at low latitudes than in the extratropics. These results are in agreement with those of *Hirota and Niki* [1985], who based their work on subjective examination of thousands of individual hodographs.

It was suggested that the sign of the correlation of horizontal velocity and vertical temperature gradient could be used to unambiguously assign a dominant horizontal direction of propagation to each sounding. A number of impressive seasonal and geographical variations were found in the dominant propagation directions determined in this manner. In mid-latitudes there is a very strong tendency for dominant eastward propagation in summer and a less pronounced westward propagation in winter. This seasonal change is in agreement with expectations based on the effects of the mean flow on IG wave propagation [e.g., *Lindzen*, 1981]. At the equatorial stations there is a very strong dominance of eastward propagation in all seasons. One possible interpretation of this result is that the wind and temperature variations in the tropical upper stratosphere are dominated by equatorial Kelvin waves.

Most of the wind and temperature variance was found to be concentrated in the largest vertical wavelengths resolved by the profiles. There was only rather weak dependence of most properties (sense of polarization, anisotropy, dominant propagation direction) on a vertical scale, except possibly at very short scales (wavelengths less than 4 km).

Any study of this nature must begin with some attempt to isolate the IG wave component of the flow in each profile. In the present work a long-term mean was removed from each profile and then a simple high-pass filter was applied in the vertical (i.e., removal of the mean and linear trend). Any other variations in wind and temperature that cause deviations from the long-term mean can contaminate the present results and thus complicate any interpretation based on IG wave propagation. In this regard it is noteworthy that the results in the extratropics seem to be somewhat cleaner in summer than in winter. Thus, for example, the dominance of clockwise rotation with height at the extratropical sites is more complete in summer than winter. Similarly, the collimation of the ensemble of profiles is much higher in summer than in winter. In the tropics, two particular sources of concern are the diurnal tide and the QBO. To examine possible tidal contamination at the equatorial stations, the present analysis was repeated but restricted to consideration of profiles taken during a 3-hour range of local time. Similarly, spurious QBO effects were reduced by repeating the analysis with attention restricted to periods with a particular phase of the QBO. In both instances the results were quite similar to those obtained using the complete data set.

The results summarized in the figures and tables of the present paper represent an attempt at a detailed climatology of those IG wave properties that can be deduced from single-station rocket data. Comparable statistics could be computed from integrations of stratospheric GCMs. A comparison of model results with the present observed climatology should be a very useful check on the adequacy of model simulation. Preliminary work with the GFDL troposphere-stratosphere-mesosphere "SKYHI" GCM has been quite encouraging [*Hamilton*, 1988] and more extensive calculations are in progress.

TABLE 12. Various Statistics at Ascension Island Computed With All the Observations and Then With Only Those Observations Taken Between 1200 and 1500 UT

	All Available Observations		Observations Between 1200 and 1500 UT Only	
Statistic	Summer	Winter	Summer	Winter
Number of profiles	366	366	210	225
rms wind amplitude, m/s	9.6	9.9	9.5	9.8
rms temperature amplitude, °C	2.8	3.0	2.8	3.0
Fraction clockwise	0.30	0.25	0.29	0.25
Mean anisotropy	4.3	4.2	4.3	4.0
Mean direction (degrees E of N)	82	87	85	88
Collimation	0.44	0.62	0.44	0.63

Acknowledgments. The author wishes to thank Jerry Cayford for his help in the initial quality control of the rocket data. He wishes to acknowledge helpful correspondence with Stephen Eckermann, who also provided copies of his own work prior to publication. He also thanks Yoshi Hayashi, Jerry Mahlman, and Li Yuan for reviewing the manuscript. Isamu Hirota and an anonymous reviewer provided useful comments.

REFERENCES

Cayford, J., and K. Hamilton, Monthly mean wind and temperature climatologies based on rocket soundings from 20 meteorological rocket stations throughout the world, *Rep., 87-5*, 44 pp., McGill Univ. Climate Group Res., Montreal, Can., 1987.

Eckermann, S. D., and W. K. Hocking, Effect of superposition on measurements of atmospheric gravity waves: A cautionary note and some reinterpretations, *J. Geophys. Res., 94*, 6333–6339, 1989.

Eckermann, S. D., and R. A. Vincent, Falling sphere observations of anisotropic gravity wave motions in the upper stratosphere over Australia, *Pure Appl. Geophys., 130*, 509–532, 1989.

Hamilton, K., The vertical structure of the quasi-biennial oscillation: Observations and theory, *Atmos. Ocean, 19*, 236–250, 1981.

Hamilton, K., Diagnostic study of the momentum balance in the Northern Hemisphere winter stratosphere, *Mon. Weather Rev., 111*, 1434–1441, 1983.

Hamilton, K., Evaluation of the gravity wave field in the middle atmosphere of the GFDL "SKYHI" general circulation model, *Tech. Doc. 273*, pp. 264–271, World Meteorol. Org., Switzerland, 1988.

Hamilton, K., and J. D. Mahlman, General circulation model simulation of the semiannual oscillation of the tropical middle atmosphere, *J. Atmos. Sci., 45*, 3212–3235, 1988.

Hartmann, D. L., The dynamical climatology of the stratosphere in the Southern Hemisphere during late winter 1973, *J. Atmos. Sci., 33*, 1789–1802, 1976.

Hayashi, Y., D. G. Golder, J. D. Mahlman, and S. Miyahara, The effect of horizontal resolution on gravity waves simulated by the

GFDL "SKYHI" general circulation model, *Pure Appl. Geophys.*, *130*, 421–443, 1989.

Hirota, I., Equatorial waves in the upper stratosphere and mesosphere in relation to the semiannual oscillation of the zonal wind, *J. Atmos. Sci.*, *35*, 714–722, 1978.

Hirota, I., and T. Niki, A statistical study of inertia gravity waves in the stratosphere, *J. Meteorol. Soc. Jpn.*, *63*, 1055–1066, 1985.

Holton, J. R., The role of gravity wave induced drag and diffusion in the momentum budget of the mesosphere, *J. Atmos. Sci.*, *39*, 791–799, 1982.

Kitamura, Y., and I. Hirota, Small-scale disturbances in the lower stratosphere revealed by daily rawinsonde observation, *J. Meteorol. Soc. Jpn.*, *67*, 817–831, 1989.

Lindzen, R. S., Turbulence and stress due to gravity wave and tidal breakdown, *J. Geophys. Res.*, *86*, 9707–9714, 1981.

Mahlman, J. D., and L. J. Umscheid, Comprehensive modeling of the middle atmosphere: The influence of horizontal resolution, in *Transport Processes in the Middle Atmosphere*, edited by G. Visconti and R. Garcia, pp. 251–266, D. Riedel, Hingham, Mass., 1987.

Miyahara, S., Y. Hayashi, and J. D. Mahlman, Interactions between gravity waves and the planetary scale flow simulated by the GFDL "SKYHI" general circulation model, *J. Atmos. Sci.*, *43*, 1844–1861, 1986.

Naujokat, B., An update of the observed quasi-biennial oscillation of the stratospheric winds over the tropics, *J. Atmos. Sci.*, *43*, 1873–1877, 1986.

Reed, R. J., The quasi-biennial oscillation of the atmosphere between 30 and 50 km over Ascension Island, *J. Atmos. Sci.*, *22*, 331–333, 1965.

Reed, R. J., M. J. Oard, and M. Sieminski, A comparison of observed and theoretical diurnal tidal motions between 30 and 60 km, *Mon. Weather Rev.*, *97*, 456–459, 1969.

Rind, D., R. Suozzo, N. K. Balachandran, A. Lacis, and G. Russell, The GISS global climate-middle atmosphere model, Part I, Model structure and climatology, *J. Atmos. Sci.*, *45*, 329–370, 1988.

Smith, A. K., and L. V. Lyjak, An observational estimate of gravity wave drag from the momentum balance in the middle atmosphere, *J. Geophys. Res.*, *90*, 2233–2241, 1985.

Vincent, R. A., and D. C. Fritts, A climatology of gravity wave motions in the mesopause region at Adelaide, Australia, *J. Atmos. Sci.*, *44*, 748–760, 1987.

K. Hamilton, Geophysical Fluid Dynamics Laboratory/NOAA, Princeton University, P. O. Box 308, Princeton, NJ 08542.

(Received January 7, 1991;
revised May 28, 1991;
accepted May 30, 1991.)